Low-Valent Si Complexes Supported by Bicyclic (Alkyl)(Amino) Carbene (MeBICAAC): Syntheses, Characterization, and Reactivity Studies

Sandeep Kumar Thakur,[a],† Sriman De,[b],† Manu Adhikari,[a],† Krishna K. Manar,[a],$ Debasis Koley*[b] and Sanjay Singh*[a]

[a]	Dr. S. K. Thakur, M. Adhikari, Dr. K. K. Manar and Prof. S. Singh Department of Chemical Sciences Indian Institute of Science Education and Research (IISER) Mohali Knowledge City, Sector 81, SAS Nagar Mohali 140306 (Punjab), India E-mail: sanjaysingh@iisermohali.ac.in
$	Present address: Department of Chemistry, University of Allahabad, Prayagraj-211002, Uttar Pradesh, India
[b]	Dr. S. De and Prof. D. Koley Department of Chemical Sciences Indian Institute of Science Education and Research (IISER) Kolkata Mohanpur, 741246 (India) E-mail: koley@iiserkol.ac.in

†These authos contributed equally to this work.

Abstract: Past one decade has witnessed the tremendous growth in the field of carbenes stabilized low-valent silicon compounds owing to very exciting properties of these molecules. Herein, we have employed a bicyclic (alkyl)(amino)carbene (MeBICAAC) to explore the low-valent chemistry of silicon compounds. The reduction of bicyclic (alkyl)(amino)carbene-SiCl4 complex, [(MeBICAAC)SiCl4] (**1**) with KC8 afforded their low-valent Si complexes, including Si(III) radical [(MeBICAAC)SiCl3] (**2**) and a complex with silicon center in a formal zero-valent state [(MeBICAAC)2Si] (**3**). Similarly, the reduction of *in-situ* generated MeBICAAC adduct of Me2SiCl2 with one equivalent of KC8 leads to the formation of [(MeBICAAC)SiMe2Cl] (**4**) complex having an unpaired electron. All these complexes have been characterized by IR, UV-Vis., NMR, HRMS, EPR and their solid-state structures were also elucidated by single crystal X-ray crystallography. Further, DFT calculations revealed the lower energy singlet state for complexes **1**, **3** and doublet state for complexes **2**, **4**.

Introduction

Silicon, the second most abundant element on the earth's crust and readily available as silica in its tetravalent state. In contrast to the tetravalent nature, the low-valent Si complexes are relatively rare nevertheless, past few decades have witnessed the progressive development in the field of low-valent silicon chemistry leading to the syntheses of new fascinating molecules.[1] The low-valent silicon complexes offer unique electronic structures and can simultaneously be used as reagents, catalysts, intermediates, and same time, providing a strong incentive to pursue this challenging endeavour.[2] Pioneering discovery of carbene stabilized halosilane by Boese and co-workers in 1995,[3] led to the subsequent agent to reduce bidentate *bis*-NHC silicon(II) cation which afforded the first cyclic six membered silylone (**C,** Figure 1).[4c] Very recently, Tan and co-workers have employed mesoionic

carbene (MIC) to stabilize Si(0) compound (**D**, Figure 1).[4d] Iwamoto and co-workers disclosed the conformationally switchable silylone using CAASi framework.[4e] Due to their unique structure, bonding, and reactivity, these complexes are of interest
rapid growth in the area of low-valent main group chemistry.
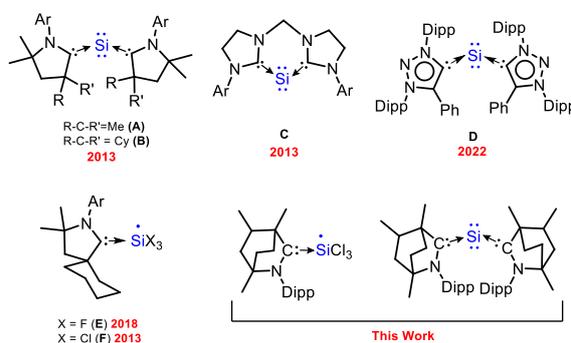
Figure 1. Known examples of mononuclear silylones and carbene stabilized radical species.

In 2013, Roesky and co-workers have synthesized the first two-coordinated Si(0) compound, 'silylone' (L:→Si←:L) using Cy/MeCAAC carbene (**A** and **B**, Figure 1) (CAAC = :C(CH2)(CR2)2N-2,6-i-Pr2C6H3, CR2 =CMe2 or C(Cyclohexyl)).[4a, 4b] Similarly, Driess and co-workers have used alkali metal-based reducing agent to reduce bidentate *bis*-NHC silicon(II) cation which afforded the first cyclic six membered silylone (**C,** Figure 1).[4c] Very recently, Tan and co-workers have employed mesoionic carbene (MIC) to stabilize Si(0) compound (**D**, Figure 1).[4d] Iwamoto and co-workers disclosed the conformationally switchable silylone using CAASi framework.[4e] Due to their unique structure, bonding, and reactivity, these complexes are of interest for the synthetic as well as theoretical chemists. Szilvási, in his computational calculations, found that low-

valent silicon complexes can outperform traditional ligands (phosphines and carbenes) towards transition metal complexation.[5] In line with these theoretical calculations, the reactivity of low-valent silicon complexes have also been explored towards Lewis acids, chalcogens and activation of small molecules such as CO_2, NH_3, H_2, C-H borylation of arenes, hydrosilylation of ketones, and in cycloaddition reactions unravelling the importance of silylones.[6]

Furthermore, the radicals and biradicals are also an important class of intermediates used in organometallic, organic, and biological processes due to their remarkable structural and electronic properties.[7] The successful isolation of triphenylmethyl radical by Gomberg was a landmark discovery that led the foundations of modern era of organic free radical chemistry.[8] Apart from this, seminal work by Sekiguchi, Kira, Lappert, Power, Bertrand, and Roesky provides valuable information about nature of persistent radicals.[9] A recent study has shown carbenes as putative ligands in providing demanding stability to these radical species to prevent them from dimerization, disproportionation or hydrogen abstraction like side reactions which are favored thermodynamically and kinetically very facile.[10] In this direction, several main-group paramagnetic molecules were synthesized using CAACs and NHCs carbenes.[9k, 9l] Roesky and co-workers have utilized π-acidic $^{Me/Cy}$CAAC to isolate [($^{Me/Cy}$CAAC)SiX$_3$] (X = F (**E**), Cl (**F**, Figure 1)) radicals,[9g, 9j] Further, the reaction of [($^{Me/Cy}$CAAC)$_2$Si] and [(^{Cy}CAAC)$_2$Si$_2$] with potassium gave unprecedented C-H activated product *via* silicon-based radical anion intermediate.[11] Apart from these monoradicals, there are some reports on silicon-based stable biradicals as well.[4b, 9e, 9f, 12]

These results emphasize that the stability of highly electron-rich silylone and silicon radical species depends upon the ambiphilic nature and steric properties of carbene. So, we became interested to explore the reactivity pattern of newly synthesized bicyclic (alkyl)(amino)carbene (^{Me}BICAAC) having better σ-donation and π-acceptance abilities.[13] Recently, we have reported the M-^{Me}BICAAC (M = Ni, Pd, Ir) complexes for cross-coupling and transfer hydrogenation reactions.[14] Also, the low-valent boron complexes were synthesized using ^{Me}BICAAC and their coordination chemistry with coinage metals were explored.[14] Herein, we have synthesized [(^{Me}BICAAC)SiCl$_4$] (**1**), [(^{Me}BICAAC)SiCl$_3$] (**2**), [(^{Me}BICAAC)$_2$Si] (**3**) and [(^{Me}BICAAC)SiMe$_2$Cl] (**4**) complexes on the platform of ^{Me}BICAAC.

Results and Discussion

Complex [(^{Me}BICAAC)SiCl$_4$] (**1**) was synthesized by an equimolar reaction of ^{Me}BICAAC and SiCl$_4$ in *n*-hexane (Scheme 1) and isolated as a white solid in 76 % yield. The ^{1}H NMR spectrum of **1** in C$_6$D$_6$ showed two septets at 3.05 and 2.95 ppm corresponding to two isopropyl groups (-C*H*(CH$_3$)$_2$) present on the ^{Me}BICAAC backbone (See ESI, Figure S1). These signals are slightly upfield compared to

the ^{Me}BICAAC (3.30 and 2.97 ppm). Other signals in ^{1}H NMR were also in accordance with the ^{Me}BICAAC unit.

Dipp = 2,6-diisopropylphenyl
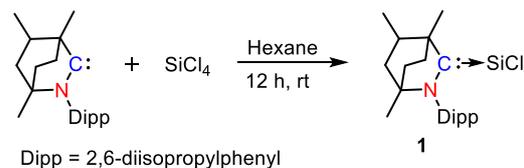
Scheme 1. Synthesis of [(^{Me}BICAAC)SiCl$_4$] complex (**1**).

The ^{13}C{^{1}H} NMR spectrum of complex **1** in the solution phase could not be recorded due to its low solubility, however in the solid state, ^{13}C and ^{29}Si NMR spectra gave indications for the formation of **1** (See ESI, Figure S2 and S3). In ^{29}Si NMR spectrum, a signal at -106.8 ppm which is significantly upfield shifted compared to the signal of neat SiCl$_4$ (-18 ppm) indicated the ^{Me}BICAAC binding to the Si center with pentacoordinated environment. The HRMS spectrum of **1** exhibited a signal at *m/z* = 443.1349 (calcd. 443.1370, which is attributed to [M-Cl-H]$^+$ (See ESI, Figure S3). Complex **1** showed a broad UV-Vis absorption band at 254 nm and was found to be thermally stable up to 196-198 °C.

Complex **1** is stable under inert conditions at room temperature. The solid-state structure of **1** was determined by single-crystal X-ray diffraction (Figure 2). It was found to crystallize in the monoclinic system with *P*2$_1$/*n* space group. Four asymmetric units of **1** crystallized in the unit cell and are held together by weak hydrogen bonding interactions (H···Cl 2.879 and 2.935 Å)[16] (See ESI, Figure S15). In the solid state, silicon atoms are located at the
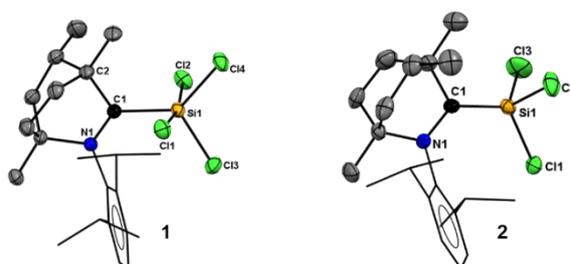
Figure 2. Single crystal X-ray structure of complexes [(^{Me}BICAAC)SiCl$_4$] (**1**) and [(^{Me}BICAAC)SiCl$_3$] (**2**). Thermal ellipsoids are set at 50 % probability. All hydrogen atoms have been omitted for clarity. Dipp groups are shown in wireframe. Selected interatomic distances (Å) and bond angles (°) for **1**: Si1-C1 1.9520(15), Cl1-Si1 2.2022(6), Cl2-Si1 2.1839(7), Cl3-Si1 2.0626(6), Cl4-Si1 2.1046(6), N1-C1 1.3128(19); C1-Si1-Cl1 84.22(5), C1-Si1-Cl2 88.12(5), C1-Si1-Cl3 118.08(5), C1-Si1-Cl4 132.35(5), Cl2-Si1-Cl1 167.82(3), Cl3-Si1-Cl4 109.51(3), for **2**: Si1-C1 1.811(3), Cl1-Si1 2.0391(12), Cl2-Si1 2.0555(14), Cl3-Si1 2.0700(14), N1-C1 1.383(4); C1-Si1-Cl1 118.06(11), C1-Si1-Cl2 112.43(12), C1-Si1-Cl3 113.85(12).

center of distorted trigonal bipyramidal (TBP) geometry where the primary coordination sphere around silicon is defined by a trigonal plane derived from C1, Cl3 and Cl4 with sum of angles around Si is 359.94° and Cl1 and Cl2 occupied the axial positions with Cl1-Si1-Cl2 bond angle of

167.82(3)°. The ^{Me}BICAAC moiety was found to bind the silicon from equatorial plane unlike the case of [(NHC)SiF$_4$] complex where NHC coordinated to silicon from an axial site.[15] Complex **1** showed deviations from ideal TBP geometry based on structural parameters τ (0.591) which should be 1 for ideal TBP and 0 for square pyramidal geometry. The Si1 atom is present on the plane of C1-Cl3-Cl4 atoms with marginal deviation of 0.027 Å. The chloride groups that occupy axial positions have longer Si-Cl bonds (Si1-Cl1 2.2022(6) and Si-Cl2 2.1839(7) Å), compared to chlorides Cl3 and Cl4 present at equatorial sites (2.0626(6) and 2.1046(6) Å, respectively). The Si1-C1 bond length 1.9520(15) Å is comparable to similar complexes with NHC-SiCl$_4$ (1.911(7) Å) [NHC = :C{N(Et)C(CH$_3$)}$_2$] and CAAC-SiCl$_4$ (1.944(2) Å) [CAAC = :C(CH$_2$)(CMe$_2$)$_2$N-2,6-i-Pr$_2$C$_6$H$_3$][3,9j] and indicated the presence of C→Si donor-acceptor single bond.

Due to the Lewis acidic nature of halogenated silicon compounds and presence of vacant d-orbitals they usually form a stable adducts with the carbenes, and are potential synthon for reduction reactions to prepare low-valent silicon compounds. In this context, we have utilized compound **1** for the synthesis of low-valent silicon complexes. The heterogeneous solution of **1** in n-hexane turned fluorescent yellow-green upon addition of an equivalent amount of KC$_8$ (Scheme 2), and [(^{Me}BICAAC)SiCl$_3$] (**2**) was obtained in 35% yield as yellow-orange crystals after the workup. The ^{1}H NMR measurements showed paramagnetic nature of the product. The HRMS spectrum of the product showed signal at m/z = 446.1626 (calcd. 446.1604), corresponding to (M+2H)$^+$ of [(^{Me}BICAAC)SiCl$_3$] (**2**) (See ESI, Figure S4), which was later confirmed by single crystal X-ray structure as well. Complex **2** showed UV-Vis absorption bands at 223, 274 and 412 nm in n-hexane solution (See ESI, Figure S11) and melts in the range of 182-184 °C.
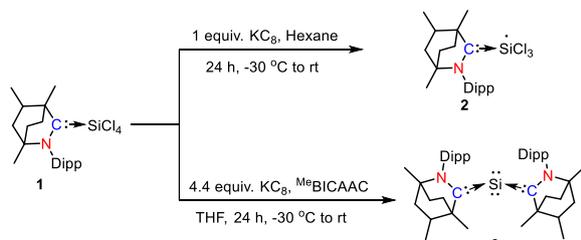
Scheme 2. Synthesis of [(^{Me}BICAAC)SiCl$_3$] (**2**) and [(^{Me}BICAAC)$_2$Si] (**3**) complexes.

The fluorescent yellow-orange solid **2** crystallized in the monoclinic crystal system with $P2_1/n$ space group with four asymmetric units present in the unit cell (Figure 2). Silicon atom is residing in a distorted tetrahedral environment attached with three chloride groups (Cl1, Cl2 and Cl3) and carbene carbon (C1). The Si1-C1 bond distance in **2** (1.811(3) Å) is shorter as compared to the corresponding distance in its precursor **1** (1.9520(15) Å). The crystal structure of **2** also revealed the existence of weak non-covalent interactions between hydrogen and chloride groups. The H···Cl distances H8B-Cl2 and H3A-Cl2 are 2.890 and 2.927 Å respectively, which are shorter than the sum of the van der Waals radii (2.95 Å), indicating the presence of significant intermolecular H···Cl interactions (See ESI, Figure S15).[16]

After the successful isolation of **2**, we made attempts for the synthesis of a Si(0) species, [(^{Me}BICAAC)$_2$Si] (**3**) by complete dechlorination of complex **1**. Such compounds were predicted by Frenking's group in 2009,[5a,5b] usually synthesized by reduction of corresponding Si(II) halides complexes.[4] Herein, we have synthesized a Si(0) species directly from a Si(IV) precursor using KC$_8$ in the presence of an additional equivalent of ^{Me}BICAAC, this methodology reduces the number of reaction steps (Scheme 2). The reaction mixture of [(^{Me}BICAAC)SiCl$_4$], ^{Me}BICAAC and KC$_8$ was stirred for 24 h in THF and a blue colored fluffy solid as [(^{Me}BICAAC)$_2$Si] (**3**) was isolated in 36 % yield after the workup. Complex **3** melts in the range of 170-174 °C. The HRMS measurements of **3** showed the signal at m/z = 651.5052 (calcd. 651.5073) for [M+H]$^+$ corresponding to the composition of **3** as [(^{Me}BICAAC)$_2$Si] (See ESI, Figure S6). The UV-Vis spectrum of **3** showed two major absorption bands at 340 and 630 nm and a shoulder at 538 nm (See ESI, Figure S12). Unfortunately, repeated attempts for NMR measurements of **3** were not successful due to uncontrolled side reactions and issues with the purity of the sample. We attribute this problem to the presence of impurities arising due to incomplete removal all chlorines from the reactant leading to the formation of [(^{Me}BICAAC)$_2$SiCl$_n$] (n = 2 or 3) complexes. The presence of signal at m/z = 683.4545 (calcd. 683.4528 for [M-2H]) in HRMS measurements (See ESI, Figure S7) corresponds to [(^{Me}BICAAC)$_2$SiCl] indicated the presence of side product.
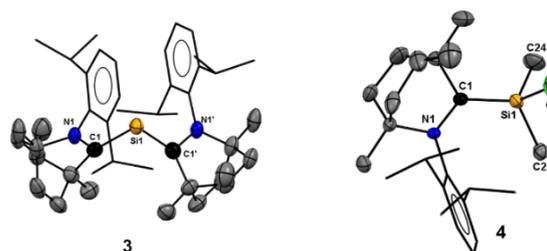
Figure 3. Single crystal X-ray structure of complexes [(^{Me}BICAAC)$_2$Si] (**3**) and [(^{Me}BICAAC)SiMe$_2$Cl] (**4**). Thermal ellipsoids are set at 50 % probability. All hydrogen atoms have been omitted for clarity. Dipp groups are shown in wireframe. Selected interatomic distances (Å) and bond angles (°) for **3**: Si1-C1 1.840(4), C1-N1 1.398(4); C1-Si1-C1' 119.0(2), N1-C1-Si1 115.1(2), for **4**: Si1-C1 1.840(4), Cl1-Si1 2.1142(15), Si1-C23 1.870(4), Si1 C24 1.877(5), N1-C1 1.392(4); C1-Si1-C24 115.3(2), C23-Si1-Cl1 102.16(13), C23-Si1-C24 105.3(2), C24-Si1-Cl1 104.01(19).

Complex **3** is highly soluble in most of organic solvents. We were lucky to obtained few crystals from the reaction mixture that corresponds to complex **3.** It was found to crystallize in the monoclinic crystal system with $C2/c$ space group (Figure 3). Silicon adopts a bent geometry where Si(0) center is coordinated with two ^{Me}BICAAC units at an angle of 119.0(2)° (C1-Si1-C1'). The Dipp groups attached to the nitrogen atoms of two ^{Me}BICAAC are oriented on the same side but twisted away from each other at an angle of 65.29° to minimize steric congestions. The Si1-C1/C1' bond distance in **3** is 1.840(4) Å which is significantly shorter than that in complex **1** (1.9520(15) Å). The C1-Si1-C1' bond angle (119.0(2)°) is

wider than that of [(^{Me}CAAC)$_2$Si], [(MIC)$_2$Si] and [(*bis*-NHC)Si] complexes (Table 1). It is interesting to note that improved Si to ^{Me}BICAAC π-back donation in [(^{Me}BICAAC)$_2$Si] (**3**) can be explained on the basis of bond length and bond angle trends when compared with [(*bis*-NHC)Si], [(MIC)$_2$Si] and [(^{Me}CAAC)$_2$Si] complexes. As a result of better π-back donation in complex **3**, the C1-N1 bond length (1.398(4) Å) is significantly elongated as compared to that of the free ^{Me}BICAAC (1.343(6)) Å.[13]

Table 1. Comparison among experimental bond lengths and bond angles for different silylones.[4]

Silylone /Parameters	[(*bis*-NHC)Si]	[(MIC)$_2$Si]	[(^{Me}CAAC)$_2$Si]	[(^{Me}BICAAC)$_2$Si]
Bond length (Si-C) (Å)	1.864(1)	1.885 (3)	1.8411(18)	1.840(4)
Bond angle (C-Si-C) (°)	89.1(1)	101.75(11)	117.70(8)	119.0(2)

Further, we have also synthesized another Si(III) radical species, [(^{Me}BICAAC)SiMe$_2$Cl] (**4**) by a single-pot reaction of ^{Me}BICAAC, Me$_2$SiCl$_2$ and KC$_8$ in THF (Scheme 3). The reaction mixture was stirred overnight under inert atmosphere of argon and filtered to remove the graphite and other insoluble species. An orange-red solid was isolated in 73 % yield after the workup. The HRMS spectrum of product showed signal at *m/z* = 404.2525 (calcd. 404.2540, [M]$^+$) corresponding to the composition as [(^{Me}BICAAC)SiMe$_2$Cl] (see ESI, Figure S8). Compound **4** is thermally stable and melts in the range of 135-137 °C. The UV-Vis spectrum of **4** showed a broad absorption peak at 465 nm (see ESI, Figure S13).
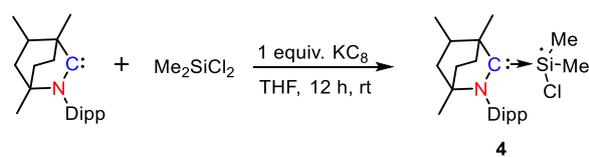
Scheme 3. Synthesis of [(^{Me}BICAAC)SiMe$_2$Cl] complex (**4**)

The molecular structure of **4** was elucidated by single-crystal X-ray crystallography. Block shaped X-ray quality crystals of **4** were grown from its concentrated THF solution at low temperature (Figure 3). Complex **4** crystallized in the monoclinic system with *P*2$_1$/*n* space group where silicon adopts distorted tetrahedral geometry. Out of four coordination sites, two were occupied by two methyl groups and the other two were occupied by ^{Me}BICAAC carbon (C1) and chloride group (Cl1). The Si1 atom is located with a distance of 0.488 Å above the plane of C1, C23 and C24 atoms.

EPR measurements

Further, in view of paramagnetic nature of complexes **2** and **4**, we have measured their X-band (9-10 GHz) EPR spectra in *n*-hexane at room temperature. The spectra obtained for **2** (Figure 4) consists of three hyperfine lines which indicates coupling with the ^{14}N nuclei in its vicinity and we have not observed any hyperfine splitting from chloride groups. Earlier Roesky and co-workers have also observed the pattern in the EPR spectrum of silicon based radical compound.[9i] Moreover, the g value, (2.004) is indicative of the formation of organic based radical. A similar pattern in the EPR spectrum of complex **4** was also observed (See ESI, Figure S14).
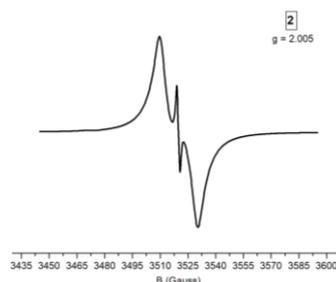
Figure 4. Experimental X-band EPR spectrum of **2** in *n*-hexane at room temperature.

DFT calculations at M06-2X/def2-SVP level were performed to illustrate the bonding environment and electronic structures of complexes **1-4** (see ESI for computational details). Computed singlet and triplet states of **1** and **3** showed that the singlet is the ground electronic state with energy differences of (ΔE_{S-T}) 85.0 and 15.6 kcal mol^{-1}, respectively, whereas **2** and **4** showed doublet electronic state. The computed bond lengths and bond angles of complexes **1-4** also showed a strong resemblance with the experimentally obtained geometrical parameters as can be seen from the alignment and superposition of the conformers (See ESI Figure S16 and Table S2).

The natural bond orbital (NBO) population analysis of complex **1** revealed that C1 is attached with Si1 through single-bond occupancy of 1.901 *e*. The C1 atom has main contribution towards electron density (ca. 78 %) in the C1-Si1 bond indicating a polar character (See ESI, Table S3).[17] The significantly shorter bond distance of C1-N1 is mainly due to the strong π-bond interaction to disrupt C1-Si1 back donation. This finding also suggest that the C1 is enclosed to the Si1 as a singlet carbene donor (C1→Si1). In complex **3**, Si1 atom is connected with C1/C1′ atoms by a single bond with electron occupancy of 1.944 *e* which are primarily located on the C1/C1′ (79%) center. Molecular orbital analysis depicted that HOMO-1 is a lone pair orbital at Si1 whereas HOMO showed a π-type orbital having larger extent towards Si1 and exhibits considerable Si-C π-bonding (Figure 5). This bonding phenomena relates with [(^{Me}CAAC)$_2$Si] complex as reported earlier[4a] and the calculated Si-C bond lengths (1.854 Å) of complex **3** are slightly shorter than the [(NHC)$_2$Si] (1.869 Å).[18] A silylone L$_2$Si: type characteristics is also described from the shapes of HOMO and HOMO-1 orbitals of complex **3**.[4a,18] For further validation, we have also calculated the first and the second proton affinities (PAs) of compound **3**. The large

value for the second PA(2) [PA(1) = 266.9 kcal mol^{-1}; PA(2) = 191.2 kcal mol^{-1}] at BP86/def2-SVP levels defend the assignment of compound **3** as a silylone.[4a] NBO calculations also revealed slightly stronger Si→C π-backdonation than Si←C σ-donation in **3**, as indicated by the NPA charge on the silicon center (q_{Si} = 0.570 *e*), however the extent is lower than in SiMe$_2$ (q_{Si} = 0.970 *e*).[4a,19] Moreover, the NBO results are further supported by the properties at the (3,-1) bond critical points (BCPs) elucidated from quantum theory of atoms in molecules (QTAIM) calculations. The important topological parameters at the BCPs are given in Table S4, ESI. The positive Laplacian value of the Si1-C1 bond in **1** [∇^{2}ρ(r); +0.146] indicated the closed-shell interaction.[20] Similarly, the dative nature of the Si1-C1/Si1-C1′ bonds in **3** are evidenced by the corresponding positive Laplacian values (+0.316/+0.316).[21]
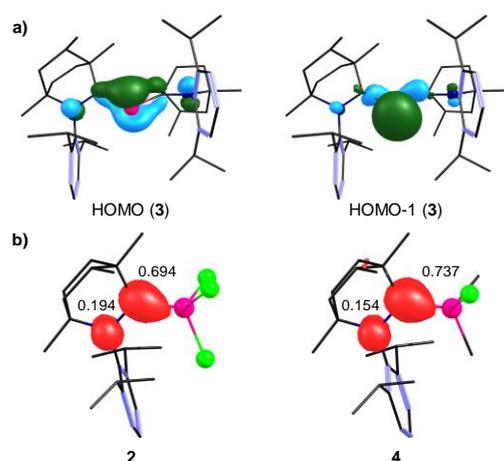
Figure 5. a) Selected KS-MOs of complex **3** (isosurface = 0.055). b) Mulliken atomic spin density plots of **2** and **4** (isosurface = 0.060 au) with selected ρ^α values. Hydrogen atoms are omitted for clarity.

In the similar way, the bonding scenario of the doublet species **2** and **4** were also investigated at same level of theory. The calculations revealed that a slight charge transfer of 0.357 *e* and 0.390 *e* occurs from the SiCl$_3$ and SiMe$_2$Cl to the ^{Me}BiCAAC fragments for **2** and **4**, respectively.[9i] This happened due to higher electronegative carbene carbon compared to silicon. Natural bond order (NBO) calculations of complexes **2** and **4** entail that in both cases C1 atom is connected to the Si1 atom by a single bond. The C1-Si1 bonding electron occupancies in **2/4** are 1.957/1.956 *e* respectively, which are highly polarized towards the C1 center [C1: 73 (α), 72 (β)/74 (α), 73 (β); **2/4**] (Table S3, ESI). The Wiberg bond indices of 0.816/0.805 in **2/4** indicates the single-bond character of the Si1−C1 bond (Table S3, ESI).[22] The Mulliken spin-density plots and values for **2/4** at the UM06-2X/def2-TZVPP//UM06-2X/def2-SVP level is represented in Figure 5 and Table S5 in ESI. The calculated spin densities confirm that the unpaired electron is mostly located on the carbene carbon [ρ^α(C1) = 0.694/0.737] for both **2** and **4**, with a small contribution from neighboring nitrogen atom [ρ^α(N1) = 0.194/0.154], whereas the spin density at Si1 [ρ^α(Si1) = 0.093/0.122 in **2/4**] atoms are negligible. The spin distribution in compounds **2** and **4** are similar to those previously reported carbene-stabilized

silicon radicals.[23] These outcomes are also supported by the NPA charges on the Si1 (1.517/1.701 *e*) and C1 (−0.386/-0.333 e) centers in **2/4**. As the C−Si bonds in complexes **2/4** are expected to be covalent from the calculated electron density [ρ(r) = 0.130/0.120] values, positive Laplacian values of +0.258/+0.249 suggest a polarized nature of the bonds (Table S4, ESI) that could be attributed to the electronegativity difference between the Si and C.[24]

In order to explain the UV-Vis spectra, we have performed the time-dependent (TD) DFT calculations at the B3LYP/def2-TZVPP/SMD//M06-2X/def2-SVP level of theory under implicit THF and *n*-hexane environment. Complex **1** exhibited the characteristic band at λ = 206.1 nm with the oscillator strength of 0.28, which is in close agreement with the experimentally observed band at λ = 254 nm (Table S6, ESI). Complex **2** showed absorption band at λ = 268.4 nm designating the *β*-HOMO–2→*β*-LUMO excitation. It is worth mentioning that *β*-HOMO-2 represents the π-orbital distributed predominantly on C1-N1 bond whereas, *β*-LUMO depicts the π-symmetric unoccupied molecular orbital centered at the carbene carbon (C1) atoms (See ESI, Figure S18). Complex **3** showed two signals at 362.5 and 586.9 nm respectively. The higher lying signal designates the HOMO−1→LUMO+1 excitation, whereas the lower-lying absorption is characterized with HOMO→LUMO excitation. HOMO-1 indicates LP orbital located on Si1 atom whereas LUMO+1 portrays a π-orbital distributed predominantly on the −Dipp group. On the other hand, HOMO describe π-type orbital through C1-Si1-C1′ area and LUMO denote π*-orbital of the carbene moiety (See ESI, Figure S17). Similarly, the (TD) DFT analysis of complex **4** gives one main excitation at 493.6 nm which is in agreement with the experimental data. The molecular orbitals of major excitations are rendered in Figure S17, ESI. The calculated g-tensor values of **2/4** (2.0021/2.0024) are also in a good correlation with the experimentally observed values (Table S7, ESI).

Conclusion

The first examples of ^{Me}BICAAC stabilized low valent silicon complexes, [(^{Me}BICAAC)SiCl$_3$] (**2**) and [(^{Me}BICAAC)SiMe$_2$Cl] (**4**) have been synthesized by reducing the Si(IV) precursor. Similarly, the complete dichlorination of [(^{Me}BICAAC)SiCl$_4$] complex (**1**) afforded a bent shaped and two coordinated Si(0) compound [(^{Me}BICAAC)$_2$Si(0)] (**3**). Complexes **2** and **4** were characterized by HRMS and solid-state structures were confirmed from the X-ray crystallography. In EPR measurements the g value and presence of three lines indicated the splitting due to ^{14}N nuclei, indicating the movement the electron density towards more electronegative carbon atom. In DFT calculations ground state doublet configurations confirmed the paramagnetic nature of **2** and **4**. DFT calculations also revealed the singlet ground state and silylone for nature of complex **3**. Further, the solid-state structure is confirmed from the X-

ray crystallography. TD-DFT calculations are in close agreements with the experimentally observed bands.

Experimental Section

General methods: All syntheses were carried out under inert atmosphere of dry nitrogen or argon using standard Schlenk techniques or a glove box. All the glassware were dried at 150 °C in an oven for at least 12 h and assembled hot and cooled in vacuo prior to use. Solvents were purified by MBRAUN solvent purification system MB SPS-800 and were used directly from the SPS system. Chemicals were purchased from Sigma-Aldrich and were used without further purification. Bicyclic (alkyl)(amino)carbene was prepared using reported procedure.[13] The ^{1}H spectrum was recorded with a Bruker 400 MHz spectrometer with tetramethylsilane (TMS) as external reference; chemical shift values are reported in ppm. FT-IR spectra of complexes (**1-4**) were recorded (in the range 4000-400 cm^{-1}) with a Perkin-Elmer Lambda 35-spectrophotometer using Nujol mull. High resolution mass spectrometry (HRMS) was performed with Waters SYNAPT G2-S. Solution state UV-Vis., spectra of complexes (**1-4**) have recorded on LABINDIA UV-Vis spectrophotometer 3000$^+$. Melting points were measured in sealed glass tube on a Büchi B-540 melting point apparatus.

Syntheses and characterization of compounds 1-4:

[(^{Me}BICAAC)SiCl$_4$] (1): In a 100 mL Schlenk flask, ^{Me}BICAAC (0.31 g, 1.00 mmol) was dissolved in *n*-hexane (20 mL), subsequently SiCl$_4$ (0.11 mL 114 μL, 1.00 mmol) was added slowly with constant stirring resulting in the formation of a white precipitate. The reaction mixture was stirred for 12 h followed by filtration to collect the white residue. The residue obtained was washed with 10 mL of *n*-hexane and dried under vacuo to afford a white powder. Colorless crystals of **1** were grown from concentrated dichloromethane solution in 3 days at -30 °C. Yield: 0.36 g, 76 %. Mp: 196-198 °C. FT-IR (Nujol mull, cm^{-1}): 2952, 2923, 2850, 2719, 1587, 1510, 1457, 1376, 1344, 1263, 1204, 1151, 1060. ^{1}H NMR (400 MHz, C$_6$D$_6$): δ = 7.06 (t, 1H, *p*Ar–H, $^3J_{H-H}$ = 8 Hz), 6.98 (d, 2H, *m*Ar–H, $^3J_{H-H}$ = 8 Hz), 3.05 (sept, 1H, C*H*(CH$_3$)$_2$, $^3J_{H-H}$ = 8 Hz), 2.95 (*sept*, 1H, C*H*(CH$_3$)$_2$, $^3J_{H-H}$ = 8 Hz), 2.28-2.21 (m, 1H) , 2.09 (s, 2H), 1.62-1.55 (m, 2H), 1.50- 1.45 (m, 5H), 1.41-1.33 (m, 2H), 1.31-1.19 (m, 5H), 1.17- 1.09 (m, 3H), 1.04-1.01 (m, 6H), 0.48 (s, 3H) ppm. ^{13}C (Solid state NMR): δ = 147.2, 144.9, 143.0, 137.0, 135.6, 130.8, 125.9, 70.6, 69.1, 47.8,47.0, 46.5, 44.7, 43.4, 39.6, 38.6, 33.7, 29.9, 29.1, 27.9, 26.9, 25.0, 23.0, 22.3, 20.3 ppm. ^{29}Si (solid state NMR) δ = -106.8 ppm. HRMS (AP$^+$): calculated for [C$_{22}$H$_{32}$NSiCl$_3$]: *m/z* = 443.1370, found: *m/z* = 443.1349 [M-H-Cl]$^+$. UV-Vis absorption a broad band at 254 nm.

[(^{Me}BICAAC)SiCl$_3$] (2): In a 100 mL Schlenk flask, an equimolar mixture of [(^{Me}BICAAC)SiCl$_4$] (1) (0.24 g, 0.5 mmol) and KC$_8$ (0.067 g, 0.5 mmol) was prepared in *n*-hexane (30 mL) at -30 °C. The reaction mixture was stirred for 24 h and filtered to remove graphite and other insoluble contents. The fluorescent yellow-green filtrate

was then concentrated and kept for crystallization at -30 °C. Yellow-orange color crystals were grown within one week. Yield: 0.15 g, 35 %. Mp: 182-184 °C. FT-IR (Nujol mull, cm^{-1}): 2954, 2925, 2854, 2727, 1458, 1377, 1261, 1161, 1094. HRMS (AP$^+$): calculated for [C$_{22}$H$_{35}$NSiCl$_3$]: *m/z* = 446.1604, found: *m/z* = 446.1626 [M+2H]$^+$. UV-Vis absorption bands at 223, 274 (broad) and 412 nm.

[(^{Me}BICAAC)$_2$Si] (3): In a 100 mL Schlenk flask, [(^{Me}BICAAC)SiCl$_4$] (**1**) (0.48 g, 1.00 mmol) was dissolved in 40 mL of THF and cooled to -30 °C for 30 minutes after this KC$_8$ (0.59 g, 4.4 mmol) was added to this solution followed by addition of 1 mmol of ^{Me}BICAAC (0.31 g). Immediately the colour of the mixture changed from colorless to intense blue. The heterogeneous mixture was further stirred for 24 h and dried and the product was extracted in *n*-hexane. Blue color crystals of X-ray quality were grown from its concentrated solution of *n*-hexane at -30 °C under inert condition. Yield: 0.23 g, 36 %. Mp: 170-174 °C. FT-IR (Nujol mull, cm^{-1}): 2959, 2920, 2857, 2730, 2340, 1461, 1376, 1302,1260, 1105. HRMS (AP+): calculated for [C$_{44}$H$_{67}$N$_2$Si]: *m/z* = 651.5073, found: *m/z* = 651.5052 [M+H]$^+$ and HRMS (ESI$^+$): calculated for [C$_{44}$H$_{64}$N$_2$SiCl]: *m/z* = 683.4528, found: *m/z* = 683.4545 [M-2H+Cl]$^+$. UV-Vis absorption bands at 340, 538 and 630 nm.

[(^{Me}BICAAC)SiMe$_2$Cl] (4): In a 100 mL Schlenk flask, ^{Me}BICAAC (0.31 g, 1.00 mmol) was dissolved in THF (20 mL) to get a clear solution, subsequently Me$_2$SiCl$_2$ (0.12 mL, 120.6 μL, 1.00 mmol) was added slowly with the constant stirring followed by the addition of an equivalent amount of KC$_8$ (0.13 g, 1.00 mmol). The colour of the reaction mixture changed from colorless to orange red. The reaction mixture was stirred for 12 h followed by filtration to remove graphite and other insoluble contents. The X-ray quality crystals were grown from its concentrated THF solution at -20 °C under inert conditions. Yield: 0.29 g, 73 %. Mp: 135-137 °C. FT-IR (Nujol mull, cm^{-1}): 2954, 2924, 2854, 2726, 1617, 1464, 1378,1321, 1260, 1251, 1175, 1095, 1029. HRMS (ESI$^+$): calculated for [C$_{24}$H$_{39}$ClNSi]: *m/z* = 404.2540, found: *m/z* = 404.2525 [M]$^+$. UV-Vis absorption band at 465 nm.

[1]   K. C. Mondal, S. Roy, H. W. Roesky, *Chem. Soc. Rev.* **2016**, *45*, 1080-1111.

[2]   C. L. B. Macdonald, B. D. Ellis, *In Encylopedia of Inorganic Chemistry*, *Vol V*, R. B. King, Ed. (*Wiley*, Hoboken, NJ, **2005**), 2781-2729.

[3]   N. Kuhn, T. Kratz, D. Bläser, R. Boese, *Chem. Ber.* **1995**, *128*, 245-250.

[4]   (a) K. C. Mondal, H. W. Roesky, M. C. Schwarzer, G. Frenking, B. Niepötter, H. Wolf, R. H. Irmer, D. Stalke, *Angew. Chem., Int. Ed.* **2013**, *52*, 2963-2967; (b) K. C. Mondal, P. P. Samuel, M. Tretiakov, A. P. Singh, H. W. Roesky, A. C. Stückl, B. Niepötter, E. Carl, H. wolf, R. H. Irmer, D. Stalke, *Inorg. Chem.* **2013**, *52*, 4736-4743; (c) Y. Xiong, S. Yao, S. Inoue, J. D. Epping, M. Driess, *Angew. Chem., Int. Ed.* **2013**, *52*, 7147-7150; (d) M. Wu, Y. He, L. Zhang, R. Wei, D. Wang, J. Liu, L. L. Liu, G. Tan, *Eur. J. Inorg. Chem.* **2022**, e202200413; (e) T. Koike, T. Nukazawa, T. Iwamoto, *J. Am. Chem. Soc.* **2021**, *143*, 35, 14332–14341; (f) M. Y.-S. Wee, S. Quek, C. S. Wu, M. D. Su, C. W. So, doi.org/10.1021/jacs.4c02807.

[5]   (a) N. Takagi, T. Shimizu, G. Frenking, *Chem. Eur. J.* **2009**, *15*, 8593-8604; (b) N. Takagi, T. Shimizu, G. Frenking, *Chem. Eur. J.* **2009**, *15*, 3448-3456; (c) Z. Benedek, T. Szilvási, *RSC Adv.* **2015**, *5*, 5077-5086.

[6]   (a) S. Yao, Y. Xiong, M. Driess, *Acc. Chem. Res.* **2017**, *50*, 2026-2032; (b) A. Burchert, R. Muller, S. Yao, C. Schattenberg, Y. Xiong, M. Kaupp, M. Driess, *Angew. Chem., Int. Ed.* **2017**, *56*, 6298-6301; (c) Y. Xiong, S. Yao, R. Muller, M. Kaupp, M. Driess, *Angew. Chem., Int. Ed.* **2015**, *54*, 10254-10257; (d) D. Wendel, T. Szilvási, C. Jandl, S. Inoue, B. Rieger, *J. Am. Chem. Soc.* **2017**, *137*, 9156-9159; (e) Y. Wang, M. Karni, S. Yao, A. Kaushansky, Y. Apeloig, *J. Am. Chem. Soc.* **2019**, *141*, 12916-12927; (f) A. Brück, D. Gallego, W. Wang, E. Irran, M. Driess, J. F. Hartwig, *Angew. Chem., Int. Ed.* **2012**, *51*, 11478-11482.

[7]   (a) M. F. Lappert, P. W. Lednor, *Adv. Organomet. Chem.*, **1976**, *14*, 345-399; (b) K. A. Bilevich, N. N. Bubnov, B. Y. Medvedev, *Russ. Chem. Bull.* **1970**, *19*, 1984-1986; (c) R. G. Hicks, *Org. Biomol. Chem.*, **2007**, *5*, 1321-1338; (d) P. Renaud, M. P. Sibi, Radicals in Organic Synthesis, *Wiley-VCH*, **2008**; (e) B. Halliwell, J. M. C. Gutteridge, Free Radicals Biology and Medicine, *Oxford University Press*, **2007**.

[8]   M. Gomberg, *J. Am. Chem. Soc.* **1900**, *22*, 757-771.

[9]   (a) A. Sekiguchi, T. Matsuno M. Ichinohe, *J. Am. Chem. Soc.* **2001**, *123*, 12436-12437; (b) A. Sekiguchi, T. Fukawa, M. Nakamoto, V. Y. Lee, M. Ichinohe, *J. Am. Chem. Soc.* **2002**, *124*, 9865-9869; (c) T. Nozawa, M. Nagata, M. Ichinohe, A. Sekiguchi, *J. Am. Chem. Soc.* **2011**, *133*, 5773–5775; (d) S. Ishida, T. Iwamoto, M. Kira, *J. Am. Chem. Soc.* **2003**, *125*, 3212-3213; (e) M. J. S. Gynane, M. F. Lappert, P. I. Riley, P. Riviere, M. Riviere-Baudet, *J. Organomet. Chem.* **1980**, *202*, 5-12; (f) H. Cox, P. B. Hitchcock, M. F. Lappert, L. J. M. Pierssens, *Angew. Chem., Int. Ed.* **2004**, *43*, 4500-4504; (g) S. Sinhababu, S. Kundu, A. N. Paesch, R. H. Irmer, D. Stalke, I. Fernández, G. Frenking, A. C. Stückl, B. Schwederski, W. Kaim, H. W. Roesky, *Chem. Eur. J.* **2018**, *24*, 1264-1268; (h) K. C. Mondal, P. P. Samuel, H. W. Roesky, B. Niepötter, R. H. Irmer, D. Stalke, F. Ehret, W. Kaim, B. Maity, D. Koley, *Chem. Eur. J.* **2014**, *20*, 9240-9245; (i) S. Sinhababu, S. Kundu, M. M. Siddiqui, A. N. Paesch, R. H. Irmer, B. Schwederski, P. Saha, L. Zhao, G. Frenking, W. Kaim, D. Stalke, H. W. Roesky, *Chem. Commun.* **2019**, *55*, 4534-4537; (j) K. C. Mondal, H. W. Roesky, A. C. Stückl, F. Ehret, W. Kaim, B. Dittrich, B. Maity, D. Koley, *Angew. Chem., Int. Ed.* **2013**, *52*, 11804-11807; (k) S. Kundu, S. Sinhababu, V. Chandrasekhar, H. W. Roesky, *Chem. Sci.* **2019**, *10*, 4727-4741;(l) C. D. Martin, M. Soleihavoup, G. Bertrand, *Chem. Sci.* **2013**, *4*, 3020-3030.

[10] Y. Wang, G. H. Robinson, *Inorg. Chem.* **2011**, *50*, 12326-12337.

[11] (a) S. Roy, K. C. Mondal, L. Krause, P. Stollberg, R. H. Irmer, D. Stalke, J. Meyer, A. C. stückl, B. Maity, D. Koley, S. K. Vasa, S. Q. Xiang, R. Linser, H. W. Roesky, *J. Am. Chem. Soc.* **2014**, *136*, 16776-16779; (b) K. C. Mondal, P. P. Samuel, H. W. Roesky, R. R. Aysin, L. A. Leites, S. Neudeck, J. Lübben, B. Dittrich, N. Holzmann, M. Hermann, G. Frenking, *J. Am. Chem. Soc.* **2014**, *136*, 8919-8922.

[12] S. Kundu, P. P. Samuel, S. Sinhababu, A. V. Luebben, B. Dittrich, D. M. Andrada, G. Frenking, A. C. Stückl, B. Schwederski, A. Paretzki, W. Kaim, H. W. Roesky, *J. Am. Chem. Soc.* **2017**, *139*, 11028-11031.

[13] E. T. Mendivil, M. M. Hansmann, C. M. Weinstein, R. Jazzar, M. Melaimi, G. Bertrand, *J. Am. Chem. Soc.* **2017**, *139*, 7753-7756.

[14] (a) S. K. Thakur, M. Kaur, K. K. Manar, M. Adhikari, A. R. Choudhury, S. Singh, *Chem. Eur. J.* **2022**, e202202237. (b) S. Chakrabortty, M. Kaur, M. Adhikari, K. K. Manar, S. Singh, *Inorg. Chem.* **2021**, *60*, 6209-6217. (c) M. Kaur, M. Adhikari, K. K. Manar, Y. Yogesh, D. Prakash, S. Singh, *Inorg. Chem.* **2024**, *63*, 1513–1523. (d) M. Adhikari, S. De, K. K. Manar, S. K. Thakur, R. S. Kamte, D. Koley, S. Singh *Eur. J. Inorg. Chem* e202400129

[15] R. S. Ghadwal, S. S. Sen, H. W. Roesky, G. Tavcar, S. Merkel, D. Stalke, *Organometallics* **2009**, *28*, 6374-6377.

[16] Y. R. Zhong, M. L. Cao, H. J. Mo, B. H. Ye, *Crystal Growth & Design* **2008**, *8*, 2283-2290.

[17] (a) K. C. Mondal, S. Roy, B. Dittrich, B. Maity, S. Dutta, D. Koley, S. K. Vasa, R. Linser, S. Dechert, H. W. Roesky, *Chem. Sci.* **2015**, *6*, 5230-5234; b) C. Mohapatra, K. C. Mondal, P. P. Samuel, H. Keil, B. Niepötter, R. Herbst-Irmer, D. Stalke, S. Dutta, D. Koley, H. W. Roesky, *Chem. Eur. J.* **2015**, *21*, 12572-12576.

[18] (a) R. Tonner, G. Frenking, *Angew. Chem., Int. Ed.* **2007**, *46*, 8695-8698; (b) R. Tonner, G. Frenking, *Chem. Eur. J.* **2008**, *14*, 3260- 3272; (c) R. Tonner, G. Frenking, *Chem. Eur. J.* **2008**, *14*, 3273-3289; (d) C. A. Dyker, V. Lavallo, B. Donnadieu, G. Bertrand, *Angew. Chem., Int. Ed.* **2008**, *47*, 3206-3209; (e) R. Tonner, G. Frenking, *Pure Appl. Chem.* **2009**, *81*, 597-614.

[19] (a) R. Kinjo, B. Donnadieu, M. A. Celik, G. Frenking, G. Bertrand, *Science* **2011**, *333*, 610-613; (b) K. C. Mondal, S. Roy, B. Maity, D. Koley, H. W. Roesky, *Inorg. Chem.* **2016**, *55*, 163-169.

[20] S. Dutta, S. De, S. Bose, E. Mahal, D. Koley, *Eur. J. Inorg. Chem.* **2020**, 638-655.

[21] (a) S. Dutta, B. Maity, D. Thirumalai, D. Koley, *Inorg. Chem.* **2018**, *57*, 3993−4008; (b) T. Mondal, S. Dutta, S. De, D. Thirumalai, D. Koley, *J. Phys. Chem. A* **2019**, *123*, 565-581.

[22] S. Dutta, T. Mondal, S. De, K. Rudra, D. Koley, *Inorg. Chim. Acta* **2019**, *485*, 162-172.

[23] (a) S. Roy, A. C. Stückl, S. Demeshko, B. Dittrich, J. Meyer, B. Maity, D. Koley, B. Schwederski, W. Kaim, H. W. Roesky, *J. Am. Chem. Soc.* **2015**, *137*, 4670-4673; (b) W. Li, S. Kundu, C. Köhler, J. Li, S. Dutta, Z. Yang, D. Stalke, R. Herbst-Irmer, A. C. Stückl, B. Schwederski, D. Koley, W. Kaim, H. W. Roesky, *Organometallics* **2019**, *38*, 1939-1945.

[24] (a) S. Kundu, S. Sinhababu, S. Dutta, T. Mondal, D. Koley, B. Dittrich, B. Schwederski, W. Kaim, A. C. Stückl, H. W. Roesky, *Chem. Commun.* **2017**, *53*, 10516-10519; (b) M. M. Siddiqui, S. Banerjee, S. Bose, S. K. Sarkar, S. K. Gupta, J. Kretsch, N. Graw, R. Herbst-Irmer, D. Stalke, S. Dutta, D. Koley, H. W. Roesky, *Inorg. Chem.* **2020**, *59*, 11253-11258.